Influence of structure on the evolution of magnetic and mechanical properties of amorphous and nanocrystalline $Fe_{85.4}Hf_{1.4}B_{13.2}$ alloy

D. Szewieczek, S. Lesz

Institute of Engineering Materials and Biomaterials, Silesian Technical University, Konarskiego 18a, 44-100 Gliwice, Poland

Abstract: The amorphous $Fe_{85.4}Hf_{1.4}B_{13.2}$ alloy is transformed into a two-phase nanocrystlline material in the optimization annealing at $T_{op}=523$ K, near to primary crystallization temperature T_{x1}. Correlations between structure and magnetic and mechanical properties in amorphous and nanocrystalline samples are studied by applying different experimental techniques. It has been shown that 1-h optimization annealing treatment at temperature T_{op} leads to a significant increase of magnetic permeability with excellent plasticity. The resulting structure is composed of αFe nanocrystlline grains with diameter of about 5 nm embedded in the amorphous matrix.

Keywords: Nanocrystalline alloys; Optimization annealing; Mössbauer spectroscopy; Magnetic and mechanical properties;

1. INTRODUCTION

In order to optimize soft magnetic properties of the nanocrystlline Fe-based alloys, many investigations have been carried out in the past decade [1-3] and various applications of these materials to electromagnetic components have been developed [4]. In these alloys, formation of a nanocrystalline phase by crystallization from the amorphous precursor can strongly improve soft magnetic properties. It has been shown that the thermal annealing at temperature close to the crystallization temperature (so-called optimization annealing) [5-9] leads to a significant increase of the initial magnetic permeability and decrease of coercive force [3, 6, 10-12]. This effect, according to the Herzer model [6, 10] can be attributed to formation of crystallites with grain size much smaller than the ferromagnetic exchange length, which leads to a random distribution of magnetic anisotropy [7-9]. The kinetic of the formation of the nanocrystalline phase depends strongly on the alloy chemistry [13].

Most investigations have been performed on the prototype Fe-Si-B-Cu-Nb soft magnetic nanocrystalline material. Research results on this class of materials showed that they exhibit excellent magnetic properties when the structure consists of αFe nanocrystalline grains with diameter of about 4-8 nm embedded in the amorphous matrix. The crystalline volume fraction should be close to 70% [14, 15]. There are only few papers on influence of the grain size and fraction of nanosized grains on the magnetic properties in other alloys (e.g. Fe-M-B, where

M=Nb, Zr, Hf) [16]. It has been shown that the improvement in the soft magnetic properties of thermally annealed nanocrystalline alloys is simultaneously accompanied by an embrittlement [15]. The brittleness is a limiting factor for many technological applications of soft magnetic materials (e.g. sensors). Hence, a better understanding of the relationship between the structure and the magnetic and mechanical properties is very important [15, 17].

Thus the goal of the paper is to study the influence of structure on the evolution of magnetic and mechanical properties of $Fe_{85.4}Hf_{1.4}B_{13.2}$ nanocrystlline ribbons obtained from amorphous precursor by the thermal annealing.

2. EXPERIMENTS

Experiments were performed on ribbons of the amorphous $Fe_{85.4}Hf_{1.4}B_{13.2}$ alloy obtained by the planar flow casting method. Ribbons had 0.024 mm thickness and 10 mm of width. Sections of ribbons of 120 mm length were annealed in the temperature range from 373÷1023 K in vacuum. The annealing time was constant and equal to 1 h, with step of 50 K. The crystallization temperatures (T_{x1} and T_{x2}) of the amorphous alloy were determined from isochronous curve ρ of samples, using the linear heating rate 0.007 K/s with measurement "in situ" [13]. The changes of tapes structures caused by the heat treatment have been investigated by the X-ray diffraction method with the use of the filtred CoK_α radiation. In order to conduct structural study, the high-resolution electron microscope (HTREM) JEM-3010 was used.

The influence of the thermal annealing on the magnetic properties of the studied samples was analyzed at room temperature by magnetic measurements. The measurements of the magnetic properties (μ_i, H_c, T_C) were carried out according to [21]. The sample after 1-h optimisation annealing at temperature T_{op}=523 K which corresponds to the maximum value of initial permeability was used for further investigations: the analysis of Mössbauer spectra, determining the αFe crystallite size and magnetisation primary curves, ductility test, fracture surface, microhardness H_v. The results of investigations of the nanocrystalline $Fe_{85.4}Hf_{1.4}B_{13.2}$ alloy were compared to the amorphous state.

The conventional Mössbauer measurements were performed by means of a constant acceleration spectrometer. The [57]Co in Rh source with an activity of about 20 mCi was used. The analysis of Mössbauer spectra made it possible to determine the average hyperfine field and volume fractions of αFe crystalline phase. The average hyperfine field was evaluated from the hyperfine field distribution obtained according to the Hesse-Rübartsch method [18].

The main grain size of the αFe phase (D) was evaluated by using Sherrer's equation [19] from the half width of (110) reflection peak [20]. Crystallite sizes are given by formula [19]: D=0.9λ/B·cosθ_B, where: λ, B and θ_B are respectively wavelength of X-ray, width and position of the peak.

The magnetization primary curves for the tapes as well as in and quenched state and after the optimization annealing treatment at temperature T_{op} were examined by a system equipped with a fluxmeter. The conditions of the heat treatment were the one-hour annealing at T_a in which μ reaches maximum value (μ_{max}) [3, 11, 21-24].

Ductility test of as-quenched and annealed ribbons was carried out by bending the tapes of 180° angle. Then value of ε=2g/h, were g-sample thickness, h-distance between micrometer jaws in moment of appearing the fracture, was determined. Fracture surfaces after decohesion in tensile testing were observed by means of OPTON DSM 940 scanning electron microscope (SEM).

The microhardness H_v was investigated with the use of the Vickers microhardness tester PMT-2.

3. RESULTS AND DISCUSSION

The X-ray tests prove that the structure of the $Fe_{85.4}Hf_{1.4}B_{13.2}$ alloy at the initial as quenched state is amorphous, which is seen on the diffraction pattern in the form of a broad-angle peak originating from amorphous phase (Fig. 1, Table 1). Obtained results of structural studies performed by X-ray diffraction are corresponding with the HRTEM micrograph and Mössbauer spectrum. The detailed analysis of these structural studies was described in [21-24].

The investigated $Fe_{85.4}Hf_{1.4}B_{13.2}$ alloy in as quenched state has excellent plasticity and in bending test the value $\varepsilon=1$ and the value of microhardness $H_v=842$ MPa (Table 1). Investigations of ribbons after decohesion in the tensile test showed their ductile character with the vein pattern morphology, typical for amorphous alloys of high ductility (Fig 2).
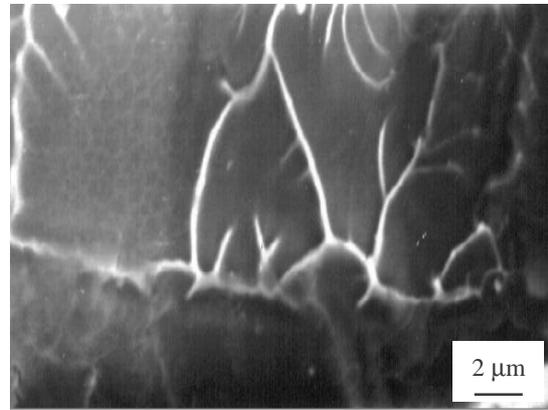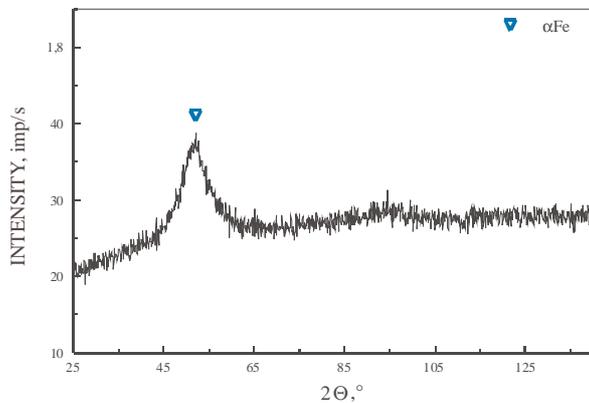
Figure 1. X-ray diffraction pattern of the $Fe_{85.4}Hf_{1.4}B_{13.2}$ alloy in as quenched state

Figure 2. SEM image of typical ductile fracture with vein pattern morphology of the amorphous $Fe_{85.4}Hf_{1.4}B_{13.2}$ ribbon in as quenched state/tensile testing.

Table 1.
The phase composition and mechanical properties (ε, H_v) of the $Fe_{85.4}Hf_{1.4}B_{13.2}$ alloy in as quenched state and after optimization annealing treatment at temperature $T_{op}=523$ K by 1 h

Heat treatment temperature, K	Phase composition of alloy	Magnetic properties	
		Plasticity ε	Microhardness H_v, MPa
as quenched	amorphous	1	842
523	amorphous+αFe	1	1076

The obtained magnetic properties i.e. initial magnetic permeability $\mu_i \approx 150$, coercive force $H_c \approx 23$ A/m and electric properties $\rho=1.120$ $\mu\Omega$m [22] allow to classify the $Fe_{85.4}Hf_{1.4}B_{13.2}$ alloy in as quenched state as a soft magnetic material. The Curie temperature determined from magnetic permeability measurements at various temperatures with continuous hating rate is equal to $T_C=509$ K (Fig. 3).

On the basis of isochronous curves of electric resistivity ρ as a function of the annealing temperature T_a, it was found out that crystallization of the investigated alloy was two-stage: primary and polymorphous [22]. This process leads to changes of the initial magnetic permeability and coercive force in the $Fe_{85.4}Hf_{1.4}B_{13.2}$ alloy [22, 23].

The highest value of the initial magnetic permeability $\mu_i \approx 239$ and almost lowest value of coercive force $H_c \approx 15$ A/m have been achieved at the annealing temperature 523 K denotes as the temperature T_{op} of optimization annealing treatment [21-24]. The increase of the initial magnetic permeability can be explain as a redistribution of the free volumes frozen-in during the production process and formation of the nanocrystalline αFe phase in the amorphous matrix. The minimum value H_c obtained at temperature 523 K can point out on the optimum value of nanocrystalline phase in the investigated alloy.

Changes in magnetic permeability achieved from the magnetization primary curves [21] the alloy in as quenched state and after optimal annealing show that the optimal annealing for the examined alloy allows to achieve $\mu_{max} \approx 37700$ at intensity of magnetic force $H_{\mu max} \approx 1$ A/m.

The thermal annealing at temperature $T_{op}=523$ K is responsible for the crystallization of the amorphous matrix. The following conclusion was drawn on the basis of the existing peak originating from the αFe phase (Fig. 4). Thus after thermal annealing at temperature T_{op}, the X-ray diffraction (Fig. 4) and HRTEM studies [21-24] showed that the structure of the samples was formed by nanocrystalline grains of αFe (about 5 nm) embedded in the amorphous matrix. The presence of the αFe crystalline phase is confirmed by the Mössbauer spectrum too [24]. From the Mössbauer spectrum analysis it was found that the average hyperfine field and the volume fraction of the crystalline phase for the investigated alloy after annealing at temperature $T_{op}=523$ K are equal 22.4 T and 1.5%, respectively [24].
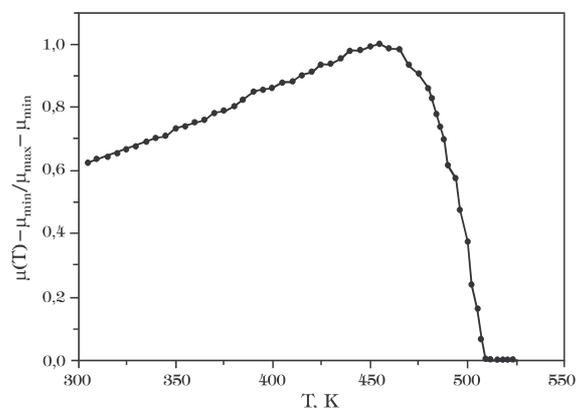
Figure 3. Normalized magnetic permeability versus temperature for the $Fe_{85.4}Hf_{1.4}B_{13.2}$ alloy (measurements in situ with heating rate 0.083 K/s)
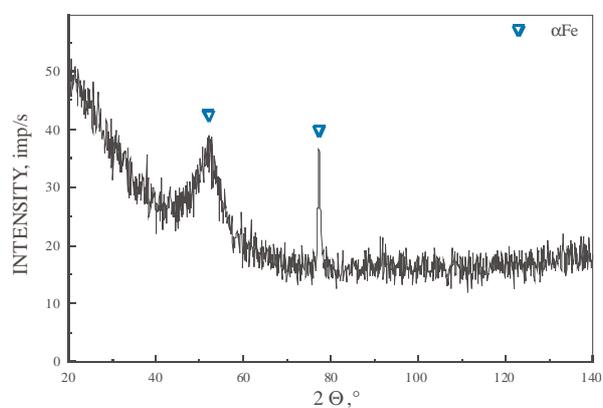
Figure 4. X-ray diffraction pattern of the $Fe_{85.4}Hf_{1.4}B_{13.2}$ alloy after optimization annealing treatment at temperature $T_{op}=$ 523 K by 1 h

Ribbons annealed at temperature T_{op} have still high ductility ($\varepsilon=1$, Table 1). The fracture morphology of ribbons after decohesion corresponds to the characteristic ductile from fracture with vein pattern (Fig. 5). But it could be seen that vein density is higher that in amorphous ribbons (Fig. 2). The microhardness of the nanocrystalline $Fe_{85.4}Hf_{1.4}B_{13.2}$ alloy is equal to $H_v=1076$ MPa (Table 1).

2 μm
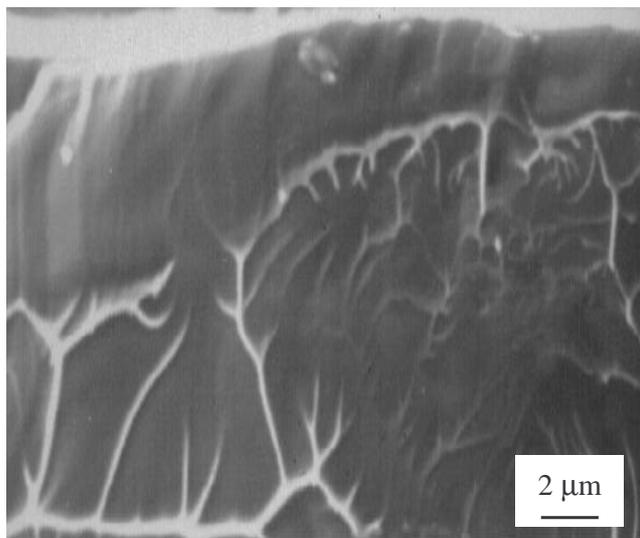
Fig. 5. SEM image of ductile vein fracture of the $Fe_{85.4}Hf_{1.4}B_{13.2}$ ribbon after optimization annealing treatment at temperature $T_{op}=$ 523 K by 1 h /tensile testing.

4. CONCLUSIONS

On the basis of the research, it was observed that the $Fe_{85.4}Hf_{1.4}B_{13.2}$ alloy in as quenched state has the amorphous structure and exhibits the following magnetic and mechanical properties: initial magnetic permeability $\mu_i \approx 150$, coercive force $H_c \approx 23$ A/m, maximum permeability $\mu_{max} \approx 19900$ and has excellent plasticity ($\varepsilon=1$) and microhardness $H_v=842$ MPa.

This alloy after optimisation annealing at $T_{op}=523$ K, close to the primary crystallization temperature T_{x1}, has the structure composed of αFe nanocrystlline grains (with diameter of about 5 nm and volume fraction 1.5%) embedded in the amorphous matrix and is characterised by excellent soft magnetic properties: $\mu_i=239$, $H_c \approx 15$ A/m) and $\mu_{max} \approx 37700$ preserving high value of plasticity ($\varepsilon=1$) and microhardness ($H_v=1076$ MPa). The maximum permeability μ_{max} of the nanocrystalline alloy type Fe-M-B, where M=Hf is higher than in other alloys with the similar chemical composition (Fe-M-B, where M=Zr, Nb) [11].

The achieved magnetic properties connected with excellent plasticity of the nanocrystalline $Fe_{85.4}Hf_{1.4}B_{13.2}$ alloy can be of significant application value, especially nowadays when more and more sensors are needed not only in the industry but also in our every day life.

REFERENCES

1. A. Makino, A. Inoue, T. Masumoto: Mater. Trans. JIM 36 (1995) 924.
2. A. Makino, T. Bitoh, A. Inoue, T. Masumoto: J. Appl. Phys. 81 (1997) 2736.
3. P. Kwapuliński, J. Rasek, Z. Stokłosa, G. Haneczok: 9-th Int. Sci. Conf. AMME 2000, Gliwice-Sopot-Gdańsk (2000) 341.
4. A. Makino, T. Hatanai, A. Inoue, T. Masumoto: Mater. Sci. Eng. A. 226-228 (1997) 594.
5. P. Kwapuliński, J. Rasek, Z. Stokłosa, G. Haneczok, M. Gigla, J. Magn. Magn. Mater. 215-216 (2000) 334.
6. G. Herzer: , J. Magn. Magn. Mater. 157-158 (1996) 133.
7. Z. Stokłosa, P. Kwapuliński, G. Haneczok, J. Rasek: J. Phys. IV 8 (1998) 51.
8. P. Kwapuliński, J. Rasek, Z. Stokłosa, B. Zegrodnik: Proc. of the 7th Int. Sci. Conf. AMME'1998 (1998) 305. (in Polish)
9. J. Rasek: Some diffusion phenomena in crystalline and amorphous metals, Silesian University Press, Katowice (2000). (in Polish)
10. G. Herzer, L.K. Varga: , J. Magn. Magn. Mater. 215-216 (2000) 506.
11. P. Kwapuliński, A. Chrobak, G. Haneczok, Z. Stokłosa, J. Rasek, J. Lelątko: Mater. Sci. Eng. C 23 (2003) 71.

12. P. Kwapuliński, J. Rasek, Z. Stokłosa, G. Haneczok: J. Magn. Magn. Mater. 254-255 (2003) 413.

13. Z. Stokłosa, J. Rasek, P. Kwapuliński, G. Haneczok, G. Badura, J. Lelątko: Mater. Sci. Eng. C 23 (2003) 49.

14. T. Kulik: Magnetically soft nanocrystalline materials obtained by the crystallization of metallic glasses, Prace naukowe, Inżynieria Materiałowa z. 7, Oficyna Wydawnicza Politechniki Warszawskiej, Warszawa (1998) (in Polish)

15. Škorvánek, P. Duhaj, J. Kováč, V. Kavečanský, R. Gerling: Mater. Sci. Eng. A 226-228 (1997) 218.

A. Chrobak, D. Chrobak, G. Haneczok, P. Kwapuliński, Z. Zwolek, M. Karolus: Mater. Sci. Eng. A 382 (2004) 401.

16. H. Chiriac, C. Hison: J. Magn. Magn. Mater. 254-255 (2003) 475.

17. Hesse, A. Rübartsch: J. Phys. E 7 (1974) 526.

A. Guinier: X-ray diffraction in crystals, in: Imperfect Crystals and Amorphous Bodies, W.H. Freeman, San Fransisco, CA (1963) 72.

18. S.N. Kene, S. Sarabhai, A. Gupta, L.K. Varga, T. Kulik: J. Magn. Magn. Mater. 215-216 (2000) 372.

19. D. Szewieczek, S. Lesz: Proc. of the 10th Jubilee Int. Sci. Conf. AMME'2001 (2001) 341.

20. S. Lesz, R. Szewczyk, D. Szewieczek, A. Bieńkowski: Proc. of the 11th Int. Sci. Conf. AMME'2002 (2002) 311-318.

21. S. Lesz, R. Szewczyk, D. Szewieczek, A. Bieńkowski: J. Mater. Proc. Techn. (in printing)

22. S. Lesz, D. Szewieczek, J.E. Frąckowiak: J. Mater. Proc. Techn. (in printing)